

Time-Dependent Density Functional Calculations of Optical Rotatory Dispersion Including Resonance Wavelengths as a Potentially Useful Tool for Determining Absolute Configurations of Chiral Molecules

Jochen Autschbach,^{*,†} Lasse Jensen,[‡] George C. Schatz,[‡] Y. C. Electra Tse,[†] and Mykhaylo Krykunov[†]

Department of Chemistry, 312 NSC, State University of New York at Buffalo, Buffalo, New York 14260-3000, and Department of Chemistry, Northwestern University, 2145 Sheridan Road, Evanston, Illinois 60208-3113

Received: August 26, 2005; In Final Form: December 9, 2005

The optical rotations for six organic molecules (verbenone, fenchone, camphor, nopinone, Tröger's base, dimethyl-cyclopropane) and the transition metal complex $[\text{Co}(\text{en})_3]^{3+}$ were calculated as a function of wavelength using time-dependent density functional theory (TDDFT). In the calculations, a realistic behavior of the optical rotation in the vicinity of an electronic transition was obtained by using a phenomenological damping parameter of the order of 0.2 eV (0.007 au). In comparison with experiment, for the molecules studied here the sign and order of magnitude of the optical rotation as well as the excitation energies were reasonably well reproduced in most computations. These findings apply to the investigated wavelength ranges typically between about 200 and 650 nm even when using comparatively small basis sets. Such calculations might therefore routinely be applied to help assigning the absolute configurations of chiral molecules. Supplementary calculations of the circular dichroism (CD) and comparison with experimental CD were used for further assessment of the optical rotation calculations. In particular, a combined study of optical rotation and CD turned out to be useful in cases where the optical rotatory dispersion in a specific energy range exhibits a considerable blue or red shift or where it is difficult to reproduce because of an interplay of several competing Cotton effects. The influence of basis set, density functional, and the damping parameter was also investigated.

1. Introduction

If a direct structure determination, e.g., by X-ray diffraction, is not feasible, the assignment of the absolute configuration of a chiral substance can be a tedious task. Computational methods for chiroptical properties (optical rotation (OR), circular dichroism (CD)) promise a convenient route to determining the absolute configuration from a comparison of easily measured chiroptical properties with calculated values.^{1,2}

A number of authors have recently pointed out that quantum chemical methods that include electron correlation can reliably predict or confirm the absolute configuration in this manner, e.g., in refs 3–6. These correlated methods are based on either *ab initio* wave-function theory (WFT) or density functional theory (DFT). Compared to DFT with standard gradient or hybrid functionals, coupled-cluster WFT based methods can be more accurate³ but they are also significantly more expensive computationally. Efficient DFT calculations of optical rotation at a single wavelength can be utilized routinely for configuration assignments within certain boundaries. For instance, the popular B3LYP hybrid functional has been shown to reproduce $[\alpha]_{\text{D}}$ values of rigid organic molecules within about 20 deg/[dm (g/cm⁻³)] on average for a set of 30 molecules.^{7,8} For this test set, nonhybrid DFT was shown to afford errors of similar magnitude but has a tendency to produce more outliers.⁹ Such uncertainties might not be acceptable in many applications. For a review of

earlier Hartree–Fock and DFT calculations of optical rotation see ref 10. A recent DFT study on a set of 65 molecules has shown that care must be taken to draw conclusions that are meaningful given the error bars of the applied basis set/functional.¹¹ From this set of molecules, it was determined that an assignment of the absolute configuration with 95% confidence would require that a computation of the specific rotation $[\alpha]_{\text{D}}$ for one of the enantiomers be within 60 deg/[dm (g/cm⁻³)] of the experimental value and the difference with experiment for the other enantiomer be >60 deg/[dm (g/cm⁻³)] at the same time.

Considering a chiroptical property over a range of frequencies might improve the predictive power of even a relatively crude calculation as long as the basis set is capable of representing at least a qualitatively correct frequency dependence of the optical rotation. Obviously, the better the agreement with experiment over a large frequency range the more trustworthy the computational results will be. Thus, results obtained with a small basis might be viewed with suspicion even if they yield a qualitatively correct optical rotation dispersion (ORD) unless there is further evidence (e.g., from CD calculations) to support the case. Presently, ORD is less often applied for combined theoretical/experimental assignments of configuration than circular dichroism but might be a useful complementary tool. In particular, in problematic cases it is beneficial to investigate both OR and CD. The advantages of a combined study of OR/CD was also pointed out, e.g., in ref 12.

In a recent paper by Giorgio et al.⁴ the authors argue that DFT even when applied with small basis sets can correctly

* To whom correspondence should be addressed. E-mail: jochena@buffalo.edu.

[†] State University of New York at Buffalo.

[‡] Northwestern University.

predict the sign pattern of the optical rotation over a range of wavelengths. Such DFT methods are routinely applicable to large molecules. In a number of studies that focused on OR calculations at multiple wavelengths,^{3–5,10,13} it has been pointed out that a calculated OR might have the wrong sign at any specific wavelength due to approximations in the calculation. However, the OR dispersion (ORD), i.e., the dependence of the OR on the wavelength λ or frequency ω of the polarized light, appears to be a very reliable indicator of the molecule's absolute configuration.^{4–6}

Particularly advantageous for structural assignments by direct comparison between theoretical and experimental OR can be the occurrence of a “fingerprint” sign pattern of the OR near an electronic excitation.⁴ In this case, the OR displays anomalous dispersion (Cotton effect) characterized by a maximum (peak) and a nearby minimum (trough) close to the absorption maximum where the OR passes through zero.¹⁴ The ORD has the opposite sign for the optical antipode. Standard linear response calculations of OR, however, do not consider a broadening of the excited-state energies and yield diverging ORs in the vicinity of electronic transitions. Though the sign pattern around the excitation is still indicative of the molecule's absolute configuration, this divergence leads to an overestimation of the OR by orders of magnitudes or might potentially result in a wrong prediction of the sign of the OR in case of competing Cotton effects. This renders the computational data somewhat artificial. An assignment of the absolute configuration based on such calculations might remain suspicious.

It is desirable to be able to simulate realistic ORD curves computationally. This might be accomplished similar to the way that CD spectra are simulated from calculated excitation energies and transition moments. For CD and other spectra usually an empirically determined line width to describe collectively, e.g., the broadening due to finite lifetime, solvent interactions, doppler effect or vibronic effects is applied to each calculated transition to obtain a spectrum that can be compared directly with experiment. Such a broadening is applied after the calculation by smoothing each CD transition with a line shape function of a certain width (typically Gaussian or Lorentzian functions are used). In principle, the ORD could simply be obtained from the Kramers–Kronig transformation of such a CD spectrum^{10,14,15} (and vice versa^{15,16}), but this might require a comparatively large number of excitations to be calculated explicitly to obtain an accurate result. Instead, we have implemented an approach for calculating the ORD directly. The computations can thus focus on a wavelength range of interest without the need for calculating all excitation energies up to a certain threshold. A “damping” parameter Γ is applied within the calculation. This approach has been embedded within a time-dependent DFT (TDDFT) treatment of the molecule. By defining complex frequencies $\omega + i\Gamma$, one obtains a complex optical rotation parameter, for which the real part remains finite even in the vicinity of an excitation. Such use of an empirical damping parameter in calculations of optical rotation and other response properties has been proposed by other authors as well. Our approach is similar to one described by Norman et al.^{17,18} and will be outlined in section 2. Our implementation was carried out in the density functional code ADF,¹⁹ which employs Slater-type basis functions and pure (nonhybrid) density functionals along with density fitting and “linear scaling” techniques to achieve high computational efficiency.^{20–22} We have applied our method as well as the Gaussian-type basis set implementation of ref 18 from the Dalton code to calculate the ORD of a number of rigid organic molecules and the transition metal

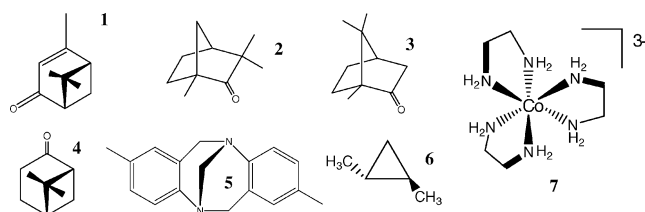


Figure 1. Molecules studied in this work.

complex $[\text{Co}(\text{en})_3]^{3+}$ shown in Figure 1. Because of the rigidity of the organic molecules it is clear that there is not a mixture of several conformations contributing to the observed ORD, which would make an assessment of the theoretical approach more difficult. For the metal complex, previous work has shown that the CD is not strongly dependent on the conformations of the chelate rings²³ and we expect this to be the case for the ORD as well. One aim of the present paper is to verify our approach with a benchmark set of molecules that are well studied already. Molecules 1–5 were recently showcased in ref 4 to demonstrate that the sign patterns of OR calculated with DFT are a reliable tool for configuration assignments. However, a damping was not applied, which makes an assessment of the accuracy of the calculations somewhat difficult. Therefore, a second aim of our paper is to demonstrate that qualitative as well as quantitative aspects of such calculations are significantly improved through the use of the damping in the response calculations. Because the damping has to be used as an input for the calculations it is important to establish values that yield reasonable agreement with experiment. A third aim is to investigate if basis sets without diffuse functions can be applied for the purpose of ORD-based configuration assignments for molecules of the type studied here, and if it is beneficial to apply an asymptotically correct Kohn–Sham potential. Finally, the cases of Tröger's base, dimethyl-cyclopropane, and Δ - $[\text{Co}(\text{en})_3]^{3+}$ are investigated in detail to highlight various interesting and/or challenging aspects of ORD calculations. Our results are presented and discussed in section 3. Our conclusions and an outlook are presented in section 4.

We will demonstrate that, by adopting a global damping parameter of the order of 0.2 eV, one can obtain reasonable ORD data from the TDDFT calculations, provided that the functional is able to predict the excitation energies accurately. Systematic errors in the excitation energies will in simple cases lead to a blue or red shift of the calculated ORD curve in comparison with experiment. We also show that comparatively small basis sets can be sufficient as long as valence excitations are of concern. Such an approach would qualify for routine applications to support experimental work. In most cases, the agreement with experimental data is not quantitative. However, for the organic molecules 1–6 shown in Figure 1 the calculations reproduce the sign and order of magnitude of the optical rotation as well as the excitation energies satisfactorily. In addition, we present calculations for the transition metal complex Δ - $[\text{Co}(\text{en})_3]^{3+}$ (7). Apart from a blue shift related to an overestimation of the lowest excitation energies the ORD is also in acceptable agreement with experiment. In cases where the absolute configuration is not known, an assignment based on such computational data could thus be made with high confidence.

2. Methodology, Computational Aspects

Computations of specific rotations at selected wavelengths λ typically between 250 and 650 nm were calculated with a locally modified version of the Amsterdam Density Functional (ADF)

program.¹⁹ We have developed a program module AORESPONSE for the DFT calculation of various frequency-dependent electric and magnetic molecular response properties.^{22,24} The module is interfaced with ADF. The inclusion of a damping parameter to calculate complex linear response properties has recently been implemented for electric polarizabilities.²² For the present work, this method has been extended to include molecular properties involving magnetic fields. Based thereupon we can calculate the complex frequency-dependent optical rotation parameter $\beta(\omega)$ for frequencies ω at or close to an electronic excitation.

A damping parameter Γ can be introduced in TDDFT linear response calculations via the linear one-particle density response function^{25–27} χ as follows:

$$\chi(\mathbf{r}, \mathbf{r}', \omega) = \sum_i \sum_a (n_i - n_a) \frac{\varphi_i^*(\mathbf{r}) \varphi_a(\mathbf{r}) \varphi_a^*(\mathbf{r}') \varphi_i(\mathbf{r}')}{\omega + i\Gamma - (\epsilon_a - \epsilon_i)/\hbar} \quad (1)$$

Here, the φ are the Kohn–Sham spin–orbitals, and the ϵ 's are their energies. We assume that no fractional occupation numbers occur. For $\Gamma = 0$, the usual undamped approach as available in various program packages^{7–9} is obtained. On the basis of eq 1, we have implemented the calculation of the complex frequency-dependent optical rotation parameter $\beta(\omega)$ into the AORESPONSE module^{22,24} following the recipes given in refs 9, 28, and 22. Compare also refs 17 and 18. Though the implementation of gauge-including atomic orbitals (GIAOs) in our code has just been completed,²¹ this approach is not deemed essential for the present work because the optical rotations obtained with a good quality standard basis in a common-gauge dipole-length formalism are not too strongly origin dependent.^{8,9,29} Future ORD studies will be based on GIAOs, however. The optical rotation parameter β is calculated from the trace of the electric-magnetic polarizability tensor G' (according to Buckingham's notation³⁰) by

$$\beta = -\frac{1}{3\omega} \sum_{\alpha \in \{x,y,z\}} G'_{\alpha\alpha} \quad (2)$$

at a given frequency ω . G' mediates the perturbation of the electric dipole moment by a magnetic field of frequency ω , and vice versa, and is calculated as a complex quantity with the help of eq 1. It is also possible to calculate the optical rotation parameter from an expression that avoids the explicit division of G' by ω in eq 2. This yields a numerically stable result for all frequencies including the limit $\omega = 0$.⁹ The specific rotation at wavelength $\lambda = 2\pi c/\omega$ is determined from the optical rotation parameter via

$$[\alpha]_\lambda = 28800 \frac{\pi^2 N_A}{\lambda^2 M} \beta \quad (3)$$

where β is in cgs units of cm^4 , M is the molar weight of the molecule in g/mol , and N_A is Avogadro's number. A related quantity is the molar rotation $[\phi]_\lambda = M[\alpha]_\lambda/100$, which we will use for the transition metal complex.

For our study, we have selected a subset of the systems recently investigated by Giorgio et al.⁴ The subset comprises compounds **1a**, **2a**, **3a**, **4a**, and **5** of ref 4 (labeled **1–5** here) as shown in Figure 1. These molecules have been selected because their experimental ORD clearly includes one or more electronic excitation. In addition to molecules **1–5**, we have studied

(1*S*,2*S*)-dimethylcyclopropane (**6**) for which one of us has, in 2002, reported a calculation of the ORD between 180 and 250 nm without damping.⁹ We have chosen **6** as an example where it is known that an asymptotically correct Kohn–Sham potential is needed to obtain the lowest excitation energy accurately. Finally, we have chosen the complex Δ -[Co(en)₃]³⁺ (**7**) for an application of TDDFT-based ORD calculations to a transition metal complex.

In ref 4, Hartree–Fock and hybrid DFT calculations on **1–5** were performed with the 6-31G* basis, which might appear inappropriate in particular because of the lack of diffuse functions. Nonetheless, for DFT the resulting ORD sign patterns and excitation wavelengths as indicated by the poles of the OR were in good agreement with experiment. In the present work, we have applied the valence triple- ζ polarized Slater-type basis “TZP” of the ADF basis set library¹⁹ for direct comparison with ref 4 in calculations of **1–5**. TZP is somewhat more flexible than the 6-31G* basis but is comparable in the sense that it lacks diffuse functions and higher angular momentum polarization functions. (However, we should point out that a Slater-type basis has a different long-range behavior that might be beneficial for the purpose of calculating valence excitations.) Such basis sets represent a rather economic choice even for larger molecules. To assess the influence of diffuse functions in the OR calculations, we have carried out additional calculations with the “Vdiff” basis of the ADF database. Vdiff consists of the TZP basis augmented with an additional set of polarization functions for each atom (d for H, f for C, O, N) and additional diffuse functions (2 sets of p functions for H and one set of s, p, d, functions for C, N, O). We have shown previously that Vdiff represents a high-quality basis for calculations of optical rotation as well as CD of organic molecules.^{9,31}

In the ADF calculations, we have applied the revised Perdew–Burke–Ernzerhof (revPBE) gradient-corrected functional^{32–35} and, for the organic molecules, the asymptotically correct “statistical average of orbital potentials” Kohn–Sham potential (SAOP) developed by Baerends et al.³⁶ SAOP may not be available in every quantum chemistry code but is considered here as a representative example of a class of asymptotically correct Kohn–Sham potentials^{37,38} that might lead to substantially improved response properties compared to regular hybrid and nonhybrid potentials. In the revPBE calculations, the 1s shells of all second-row atoms were kept frozen in the calculations. For the SAOP calculations, an all-electron basis had to be employed instead due to technical reasons related to the way the potential is implemented in the ADF code. All optical rotations were calculated on the basis of optimized geometries of the molecules. For **1–5** optimizations were carried out at the revPBE/TZP level. The structure of **6** was taken from ref 9, the structure of **7** from ref 23. As in previous work,⁹ the exchange-correlation kernel of the adiabatic local density approximation (ALDA) has been applied. Te Velde et al.'s numerical integration method³⁹ with an accuracy parameter of 4.5 has been employed in all computations along with analytical electric and magnetic dipole moment integrals for the response calculations. For the determination of electronic excitation energies and rotatory strengths the program code described in refs 20 and 31 was used, which is part of the ADF package. For **7** solvent effects were considered by applying the COnductor-like Screening MOdel of solvation (COSMO).^{40,41} CD spectra were simulated from calculated excitation energies and rotatory strengths using the method described in ref 31. We have used a uniform Lorentzian broadening characterized

by a line width at half peak height of Γ of the same order of magnitude as the damping parameter used in the ORD calculations.

For a comparison of SAOP and revPVE with hybrid DFT results, calculations were further carried out for selected cases using the Dalton program.⁴² We have used the Gaussian-type basis sets aug-cc-pVDZ and 6-311++G** as included in the Dalton basis set database and employed the B3LYP hybrid functional⁴³ as implemented in the Dalton code.

The value for the damping parameter Γ is obviously of importance if quantitative agreement with the experimental magnitudes of the OR around an excitation wavelength is of interest. After a few test calculations we have settled on a value of 0.007 atomic units (0.2 eV) for most calculations. This value is of the same order of magnitude as the line width parameter that we and others have previously employed in the simulation of CD spectra^{31,44} of a number of organic molecules. For **5**, a range of values for Γ has been employed after the calculations indicated that 0.007 au might be too small for this system. For **6**, calculations with $\Gamma = 0.009$ au yielded almost exact agreement of the ORD with experiment. If there is further spectroscopic information available, it should be possible to obtain reasonable values for Γ , for instance from UV-vis and/or CD spectra.

Experimental ORD curves were scanned from refs 4 and 45 and digitized for subsequent use in our plotting software.

3. Results and Discussion

Overall Performance of the DFT Calculations for the Organic Molecules. Figures 2–4 display the ORD for the organic molecules shown in Figure 1 obtained with and without damping, based on calculations with the SAOP potential. The experimental ORDs are also shown. The ORD curves for **1–5** that we obtained with the revPBE functional and the TZP basis are available in the Supporting Information. For compounds **1–4**, the agreement with experiment is better when using the SAOP potential, resulting in a corresponding Cotton effect that is shifted to shorter wavelengths as compared to the revPBE results. Such an influence of the SAOP potential was expected because it was designed to correct for the sometimes too small HOMO–LUMO gaps found using regular local and gradient corrected density functionals.³⁶ In ref 4, a pole of the OR of **1** was obtained with the B3LYP hybrid functional near 350 nm, which is only approximately 0.1 eV higher in energy than our SAOP results. In comparison, Hartree–Fock results from ref 4 predicted the pole at about 265 nm—more than 1 eV too high. The SAOP/TZP calculations performed here with $\Gamma = 0$ for molecules **2–4** are also in good agreement with the B3LYP calculations of ref 4. For **5** there are differences that will be discussed below.

The calculated ORs based on the damping agree very well with the experimental data for compounds **1–4**, **6**, and to a lesser extent **5** (Tröger's base). In all cases, the choice of the damping parameter yields the correct order of magnitude for the OR. For very short wavelengths, discrepancies in the magnitudes by about a factor of 2 are obtained in some cases, e.g., for **3**. It should be noted for comparison that, for instance, a factor of 2 deviation between theory and experiment for absorption and CD intensities is not uncommon. For some of the molecules, the experimental OR curves do not exhibit the Cotton effects predicted by the computations. Again, this occurs at very short wavelengths and might be due to calculated excitations having a too low energy, a lack of experimental sensitivity at short wavelengths, or a combination of these factors

and other approximations used in the computations. In addition to the approximate treatment of electron correlation by DFT as well as DFT self-interaction errors, neglected solvent effects and vibrational corrections are likely to contribute to the discrepancy between theory and experiment. Furthermore, the value of Γ is likely to vary, typically increasing as the energy of the excited state increases. We have not included this in our modeling as it would require additional information not generally available.

An important conclusion can be drawn regarding the necessity of using a basis set with diffuse functions. For the set of molecules **1–6**, the OR at 589.3 nm is improved significantly by adding diffuse functions in all cases (see Supporting Information). For the ORD shown in Figures 2–4, differences can be observed regarding the exact location of the Cotton effect as well as the magnitudes. For instance, the lowest excitation energies for **6** are noticeably too high, the lowest by about 0.25 eV, when the TZP basis is used owing to the Rydberg-like character of the excitations. A much better ORD is calculated with the Vdiff results. With $\Gamma = 0.009$ au the ORD is in very good agreement with experiment. Qualitatively, the results do not change much by the diffuse basis. In particular for the systems with low-energy valence transitions, both the polarized valence triple- ζ and the much larger diffuse basis yield similar results when compared visually with each other and experiment. This explains why the sign patterns of the ORD from ref 4 obtained with the B3LYP functional and the rather inflexible 6-31G* basis were in agreement with experiment.

Despite the fact that the agreement of theory and experiment is not quantitative in most cases, the calculated ORD curves appear to be very reasonable. The sign, order of magnitude, and the location of the Cotton effects (where an excitation is clearly separated energetically from others) are reproduced correctly. Thus, TDDFT calculations including a damping parameter appear as a promising tool for the purpose of assigning an absolute configuration as well as to investigate the structural (geometry and electronic structure) origin of the optical activity.

Comparison of Optical Rotation and Circular Dichroism Calculations for Molecules 1–4. For molecules **1–4** CD data and/or spectra are available in the literature. Pulm et al.⁴⁶ have in 1997 carried out a combined experimental/theoretical study of the CD of **2** and **3** and assigned their spectra. A CI-singles calculation based on DFT orbitals (dubbed “DFT/SCI” by the authors of ref 46) did yield good agreement with the experimental gas-phase spectra shown in Figure 5. Because the experimental spectra were reported on an electronvolt scale, simulated theoretical spectra are shown here also on an energy scale instead of wavelengths. We have performed calculations at the SAOP/Vdiff and at the B3LYP/6-311++G** level. An expected common feature of the CD of **2** and **3** is the carbonyl $n \rightarrow \pi^*$ CD-band centered around 4.21–4.28 eV (295–290 nm), which, however, has the opposite sign in the two compounds. The calculated excitation energies at the SAOP/Vdiff level are 4.22 eV/294 nm for fenchone (**2**) and 4.26 eV/291 nm for camphor (**3**), respectively, in excellent agreement with experiment. Higher-energy CD bands that were assigned in ref 46 as $n \rightarrow$ Rydberg as well as $\sigma \rightarrow \pi^*$ (the latter between 7.0 and 7.5 eV) appear in the experimental spectra above 6 eV (below 200 nm). Thus, the excitation that causes the anomalous dispersion of the ORD for **2** and **3** at wavelengths larger than 200 nm is well separated from other excitations. This leads to a comparatively simple behavior of the ORD within the experimentally accessible wavelength range despite the fact that the optical

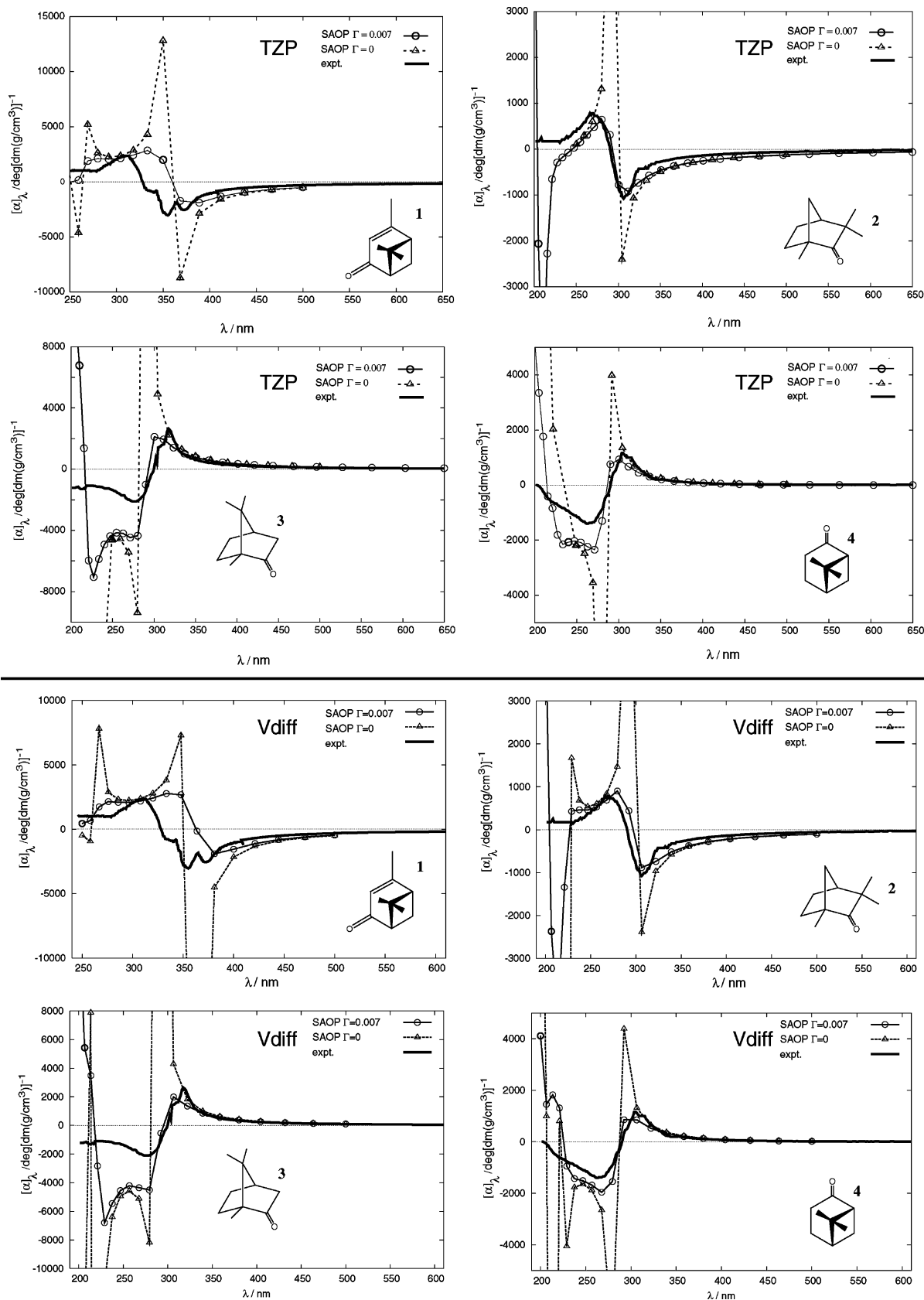


Figure 2. Specific optical rotations $[\alpha]_{\lambda}$ of compounds 1-4 as a function of the wavelength λ , calculated at the SAOP level with ($\Gamma = 0.007$ au) and without damping. Upper panel: TZP basis. Lower panel: Vdiff basis. Lines connecting the calculated values have been added to guide the eye. Experimental data from ref 4, recorded in hexane.

rotation at all wavelengths is influenced by higher lying excitations as well. Any influence of errors affecting the computation of these excitations are apparently well enough balanced not to obscure the ORD in the UV/vis range.

In the DFT calculations with the diffuse basis sets, many transitions contribute to the CD of 2 and 3 in the energy range above 6 eV/below 200 nm. For Figure 5 we have calculated the lowest 50 excitations to cover an energy range up to about

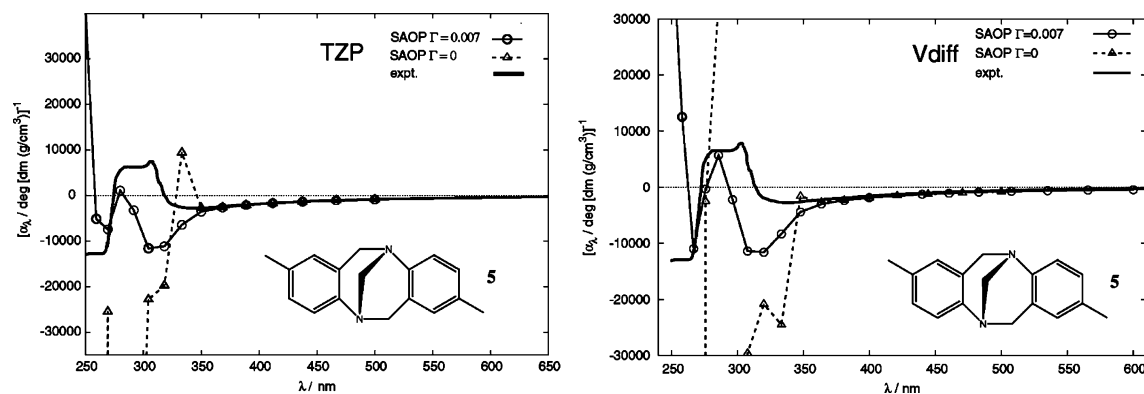


Figure 3. Specific optical rotation $[\alpha]_{\lambda}$ of compound **5** (left, SAOP/TZP; right, SAOP/Vdiff) with ($\Gamma = 0.007$ au) and without damping, as a function of the wavelength λ . Experimental data from ref 4.

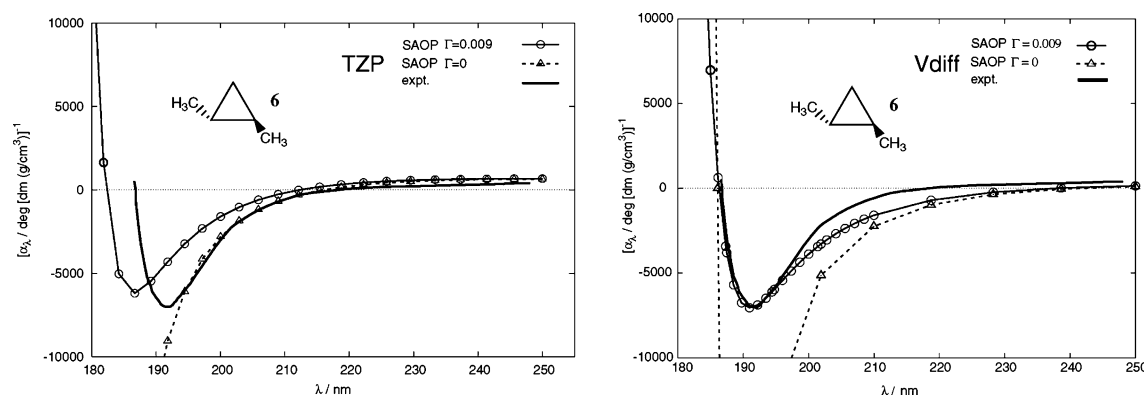


Figure 4. Specific optical rotation $[\alpha]_{\lambda}$ of compound **6** (left, SAOP/TZP; right, SAOP/Vdiff) with ($\Gamma = 0.009$ au) and without damping, as a function of the wavelength λ . Experimental data from ref 45.

9 eV. Separate spectra including the calculated excitation energies and the rotatory strengths can be found in the Supporting Information. For fenchone (**2**) the calculated spectra are in rather good agreement with each other and with experiment. The SAOP/Vdiff spectrum for camphor (**3**) affords a strong negative CD band around 5.8 eV that is not present in the well-resolved experimental spectrum. This CD band was not obtained in the DFT/SCI calculations in ref 46; however, the calculations differ from ours in the theoretical level as well as the applied basis set. The presence of this negative CD band is likely to be responsible for the overestimation of the negative OR in the range 300–200 nm (4.1–6.2 eV) by the calculations (see Figure 2). The B3LYP/6-311++G** calculation is also not in particularly good agreement with the experiment. The CD bands between 5 and 7 eV appear to be considerably red-shifted. It is interesting to note that the SAOP/Vdiff spectrum for camphor rather resembles the experimental spectrum of norcamphor (which is also shown in Figure 5). It is tempting to make deficiencies in the density functionals responsible for differences between theory and experiment in the higher energy range of the spectrum. Even though the calculated spectrum does suggest that at least some of these excitations might be too low in energy, it should be pointed out that without considering vibronic effects, it can be difficult to make direct comparisons between calculated and experimental CD spectra. For instance, in a recent paper⁴⁷ it was concluded that a “spurious” CD band calculated for dimethyloxirane is not visible in the experiment because the calculations showed that it is spread over a range of more than 1 eV. Therefore, it is overshadowed by other transitions once vibronic effects are considered in the calculation. A similar mechanism could be at work here. This would simply mean that calculated “vertical-only” transitions might in principle not be capable of reproduc-

ing the experimental spectrum very well. We are presently investigating this problem, which, however, requires a significant computational effort.

A CD spectrum for (–)-verbenone (**1**) in the range 280–380 nm was reported by Takeya et al. in 1977.⁴⁸ Within this range of wavelengths the experimental spectrum affords a single negative CD band centered at about 322 nm (3.85 eV), which is noticeably lower in energy than the pure carbonyl $n \rightarrow \pi^*$ transition of **2–4**. The nonhybrid DFT calculations underestimate the excitation energy, as already mentioned. This underestimation appears in Figure 2 in form of a red shift of the ORD curves. The calculated SAOP/Vdiff energy for the lowest transition is 3.43 eV/361 nm. As for **2** and **3**, this transition is well separated from others transitions. The next transition is calculated at 4.70 eV/264 nm. The corresponding (less intense) Cotton effect in the ORD is clearly visible in the calculations likely because of the red shift of the ORD but probably just below the accessible wavelength range in the experiment (see experimental ORD in Figure 2). A calculation performed at the B3LYP/6-311++G** level yields excitation energies of 3.56 and 5.09 eV, which would improve the ORD somewhat. Both methods yield a rotatory strength of about -9×10^{-40} cgs units for the lowest-energy transition.

CD data for nopinone (**4**) was published in 1972 by Hirata.⁴⁹ Unfortunately, only the wavelengths and magnitudes of the CD band maxima were reported numerically because of the limited wavelength range of the spectrum (between about 230 and 340 nm). A representative spectrum was shown in ref 49 for the closely related compound 10 β -pinan-4-one (**8**), which affords a negative CD band from the carbonyl $n \rightarrow \pi^*$ transition centered around 285 nm. For nopinone (**4**) the CD of the $n \rightarrow \pi^*$ transition is positive instead. The signs of the CD both for **4** and **8** are in agreement from what would be predicted from

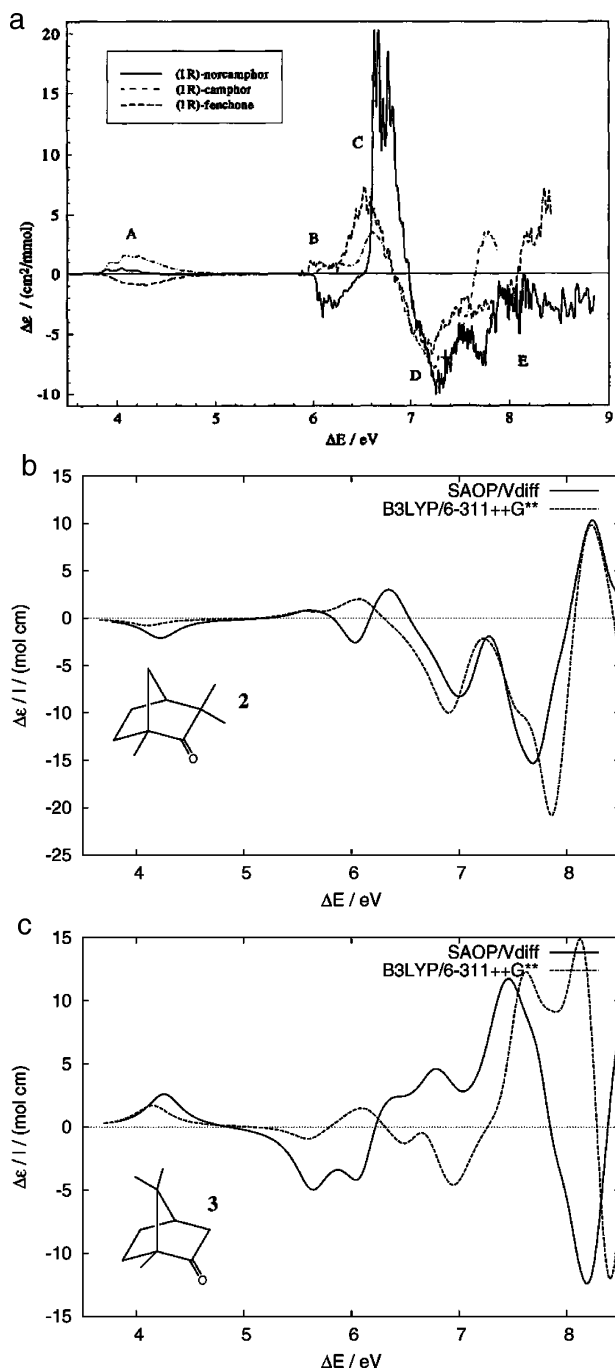


Figure 5. Circular dichroism of **2** (1*R*)-fenchone) and **3** (1*R*)-camphor). Panel a: experimental data from ref 46, reprinted with permission from Elsevier. Panel b and c: simulated CD spectra using a Lorentzian broadening with a line width of $\Gamma = 0.007$ au (0.2 eV).

the Octant rule.⁴⁹ As expected, similar to **2** and **3** the calculated CD for **4** at the SAOP/Vdiff level shows that the carbonyl $n \rightarrow \pi^*$ transition is well separated from higher-energy transitions (which are predicted at 5.5 eV and higher). The calculated energy of the $n \rightarrow \pi^*$ transition is 4.36 eV or 285 nm. This value is in very good agreement with experiment where a single CD peak was found at 283 nm with methanol as the solvent and a double peak at 292 and 284 nm, respectively, with isooctane as the solvent. The magnitude of the simulated CD intensity for this transition is also in reasonable agreement with the experimental data reported by Hirata when using a Lorentzian broadening with a line width of 0.007 au (0.2 eV). From the calculated rotatory strength of $+5.6 \times 10^{-40}$ cgs units, we obtain $\Delta\epsilon_{\max} = +1.6$ L/(mol cm) for the carbonyl $n \rightarrow \pi^*$

transition whereas experimentally $\Delta\epsilon_{\max} = 1.3$ L/(mol cm) for the methanol spectrum. The agreement of the calculated and experimental data for the carbonyl transition rationalizes the good agreement of the calculated and experimental ORD for compound **4**. As in the case of camphor (**3**), though somewhat less pronounced, the ORD of **4** indicates that the intensity of higher lying transitions with negative CD might be overestimated in the calculations and somewhat red-shifted. For instance, a sign change of the calculated ORD in Figure 2 indicates electronic transitions around 225 nm (5.5 eV, in agreement with the calculated CD) whereas the experimental ORD suggests that these transitions are closer to 200 nm (6.2 eV).

Overall, we find that for molecules **1–4** the ORD within the UV–vis range is clearly dominated by the sign and intensity of the lowest CD transition. By comparison with experiment, it is found that not only the ORD but also the CD is reasonably well reproduced in the calculations. With the help of the CD some of the differences between calculated and experimental ORD can be rationalized. For instance, for verbenone (**1**) an underestimation of the lowest excitation energy yields the noticeable red shift of the ORD curve visible in Figure 2. For camphor (**3**) a strong negative CD band around 5.8 eV seems to be the cause for the overestimation of the optical rotation between 300 and 200 nm.

Next, we will discuss molecules **5** and **6** and the metal complex **7** in more detail. The influence of approximations in the basis set and the density functionals will be investigated. For Tröger's base (**5**) and the metal complex $[\text{Co}(\text{en})_3]^{3+}$ we will again demonstrate how additional calculations of the CD spectrum can help to assess the accuracy of the OR computations and significantly increase the trustworthiness of the calculated optical rotation data (and vice versa).

Tröger's Base. Upon visual comparison, for Tröger's base (**5**), the quality of the calculations appears to be less good than for the other organic molecules. The positions of the peaks and troughs of the OR are not as accurately reproduced (Figure 3). The magnitude of the peak around 300 nm that is visible in the experiment is shifted to shorter wavelengths. Its magnitude appears to be strongly underestimated with the TZP basis. Using the diffuse Vdiff basis offers a clear improvement here. The trough at 350 nm is also shifted to shorter wavelengths in the calculations and strongly overestimated in magnitude. On the other hand, the calculated ORD above 350 nm agrees well with experiment. As pointed out in refs 4 and 50, it is difficult to calculate the long-wavelength limit of the OR for Tröger's base. The lowest-energy CD band is positive, which therefore is expected to yield a large positive contribution to the OR at long wavelengths. However, $[\alpha]_D$ is negative. The magnitude and the sign of the OR at long wavelengths is therefore balanced by competing Cotton effects, in particular in the 250–350 nm region. The Hartree–Fock method does not yield the correct sign of $[\alpha]_D$, which indicates that electron correlation is important to achieve this balance. The negative $[\alpha]_D$ is dominated by the strong negative CD bands in the 250–350 nm region instead of the lowest-energy transition itself. We have confirmed this by calculating a number of low-energy transitions and their rotatory strengths.

The calculated wavelengths for the five lowest-energy transitions at the SAOP/TZP level are 330, 310, 301, 299, and 290 nm, with rotatory strengths of +9.4, -4.9, +4.4, -19, and -33 (in 10^{-40} cgs units). These, and data for the 5 lowest-energy transitions of the other molecules, are also collected in the Supporting Information. Adding diffuse functions to the basis

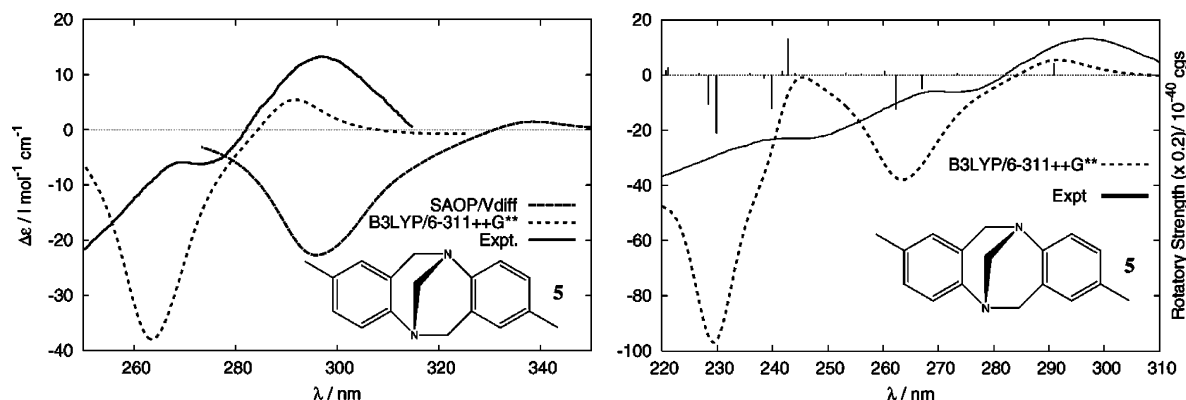


Figure 6. Low-energy part of simulated and experimental CD spectra of Tröger's base (**5**). Experimental data from ref 45. Simulated spectra using a Lorentzian broadening with a line width of $\Gamma = 0.0048$ au (0.13 eV). Left panel: comparison of SAOP/Vdiff and B3LYP/6-311++G** with experiment. Right panel: comparison of B3LYP/6-311++G** with experiment for a larger range of wavelengths. Calculated excitation energies and rotatory strengths are indicated by vertical bars.

set does not change the CD spectrum qualitatively, though using the Vdiff basis has some effect on the rotatory strengths and slightly red-shifts the spectrum. The calculated transitions are now at 337, 314, 305, 302, and 294 nm with rotatory strengths of +8.6, -3.5, +6.8, -27, and -36. Both calculations predict a sign pattern of the rotatory strengths for the lowest-energy excitations of Tröger's base that is in agreement with Hartree-Fock/6-31G* results from ref 50. A simulated CD spectrum also reproduces the correct pattern of low-energy CD bands when compared with experiment (Figure 6). An inspection of literature data⁵¹ for the CD spectrum of **5**, however, reveals that the SAOP calculation underestimates the energy for the lowest-energy excitation by about 0.4 (TZP) to 0.5 (Vdiff) eV. The experimental value was reported at 33 600 cm^{-1} or 298 nm. It is obvious that a quantitative agreement with experiment for the ORD would require an accurate description of both the excitation energies and the magnitude of each individual Cotton effect in the energy range up to about 5 eV (250 nm) and perhaps higher.

In ref 4, the hybrid DFT calculations for compound **5** appeared to predict a strongly blue-shifted undamped ORD. In our SAOP calculations, on the other hand, the excitation energies are red-shifted when compared with experiment. To investigate if deficiencies of the SAOP potential are responsible for the red shift, we have calculated a number of lowest CD transitions also with the B3LYP hybrid functional, using the 6-311++G** basis. Here, the lowest-energy transition is calculated at 4.26 eV or 291 nm, which is only a 0.1 eV overestimation of the experimental value (298 nm). Apart from an additional 0.1 eV blue shift due to missing diffuse functions, CD spectra obtained with B3LYP and other Gaussian-type basis sets such as SVP, 6-31G* and 3-21G* spectra are very similar and therefore not shown. In Figure 6 it can be seen that SAOP and B3LYP yield the same shape for the low-energy range of the CD spectrum, which qualitatively agrees with the experimental one. The line width has been decreased compared to the CD spectra of **2** and **4** (Figure 5) to be able to show the lowest-energy CD peak. With $\Gamma = 0.2$ eV the peak would hardly be visible in the simulated spectra. When a Gaussian broadening of 0.2 eV is used instead of the Lorentzian broadening, the lowest-energy CD peak becomes significantly more intense and agrees better with experiment in both the B3LYP and the SAOP calculations. However, as already mentioned, the SAOP potential underestimates the lowest excitation energies. It is known that different density functionals have shortcomings for different molecules. Obviously, the SAOP potential has difficulties describing the lowest excitation energies of Tröger's base (**5**)

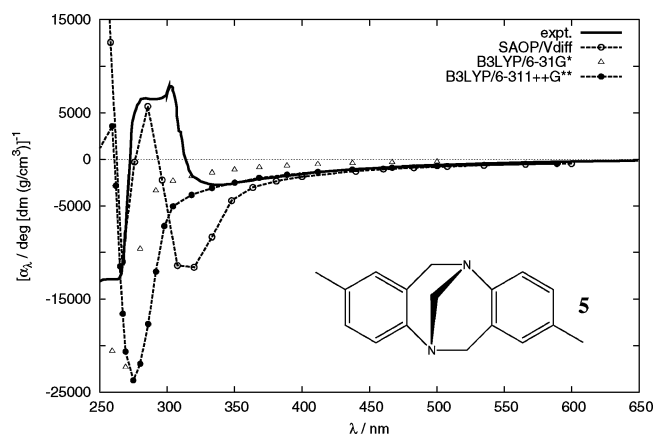


Figure 7. Specific optical rotation $[\alpha]_D$ of compound **5**. Comparison of SAOP/Vdiff (same data as in Figure 3) with the B3LYP hybrid functional using the 6-31G* and 6-311++G** basis sets. $\Gamma = 0.007$. Experimental data from ref 4 recorded in hexane.

correctly. On the other hand, in the B3LYP spectra the CD intensity appears to be overestimated quite strongly for transitions other than the lowest-energy one, which is expected to have an impact on the calculated ORD.

To investigate this issue, we have carried out hybrid-DFT calculations of the OR with a damping parameter of $\Gamma = 0.007$ au using the method of Norman et al.¹⁸ as implemented in the Dalton code. The results are displayed in Figure 7 together with the experimental and the SAOP/Vdiff data. Though the CD of Tröger's base in the low-energy region calculated with B3LYP is superior to the SAOP/Vdiff results, one can see that the OR is in reasonable agreement with experiment only for wavelengths > 350 nm but not in the region between 250 and 350 nm. The positive Cotton effect of the lowest-energy transition is not at all visible in the B3LYP calculation of the ORD when damping is included. This must be due to a superposition of Cotton effects that are close in energy. Thus, the hybrid functional is not better performing here than SAOP for the ORD of Tröger's base. For comparison with ref 4, results obtained with the 6-31G* basis are also shown. They are qualitatively similar to the ones obtained with the diffuse basis in the sense that they produce a very similar dispersion of the OR. However, at wavelengths > 350 nm the small basis severely underestimates the magnitude of the specific rotation. The $[\alpha]_D$ value for B3LYP/6-31G* is -165 $\text{deg}/[\text{dm} (\text{g}/\text{cm}^3)]$ (from ref 4) compared to the experimental specific rotation of -267 $\text{deg}/[\text{dm} (\text{g}/\text{cm}^3)]$. The SAOP/TZP $[\alpha]_D$ result, on the other hand, is too large (-537 without damping). The $[\alpha]_D$ results with the diffuse basis sets are very

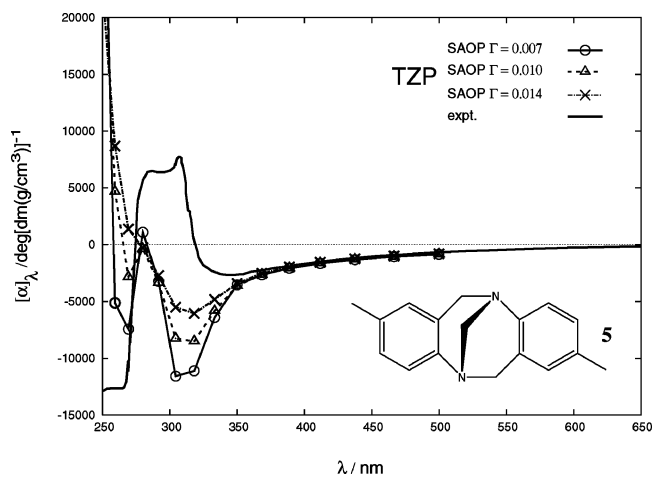


Figure 8. Specific optical rotation $[\alpha]_{\lambda}$ of compound **5** as a function of the wavelength λ , calculated at the SAOP/TZP level using different damping parameters. Experimental data from ref 4 recorded in hexane.

similar (SAOP/Vdiff, -479.6 ; B3LYP/6-311G**, -468.9), both much larger in magnitude than the experimental value. From the ORD curves and the CD spectra it is clear that the agreement of the OR at 589.3 nm for the two functionals is rather accidental.

As already mentioned, the authors of ref 4 concluded that their B3LYP/6-31G* ORD curve (calculated without damping) for **5** is qualitatively correct regarding its sign pattern but significantly blue shifted. However, the direct comparison with experiment was seriously hampered by the huge variations of the calculated values in the vicinity of the excitation energies. The rather accurate CD spectrum, the good agreement of the ORD in the region >350 nm with experiment, and the lack of an ORD peak in the 250 – 350 nm region in our B3LYP computations with damping indicates that the calculated ORD curve is not simply blue shifted.

Another influence on the agreement between theory and experiment for **5** could be the choice of the damping constant. In Figure 8 we compare the calculated OR of compound **5** for different values of Γ . For reasons of computational efficiency we have chosen the TZP basis for this comparison. Because of the overestimation of the troughs of the ORD in all DFT calculations on **5**, a larger damping parameter might seem to be appropriate. As seen in Figure 8, increasing Γ indeed reduces the OR magnitude between 300 and 320 nm but also leads to less structure of the OR at shorter wavelengths, which is not the desired outcome. The *qualitative* features of the calculated ORD are not changed by varying the damping parameter within reasonable limits. (This might be seen as an advantage because this makes Γ less suitable as a “fudge factor”.) If the transitions that influence the OR in this energy range have very different line widths, it might be necessary to employ a frequency-dependent damping parameter to reproduce the ORD between 250 and 350 nm more accurately.

Dimethylcyclopropane. Dimethylcyclopropane (**6**) has previously been studied by one of us in ref 9. SAOP calculations indicated that a calculation with damping should yield excellent agreement with experiment. Figure 4 shows that this is indeed the case. Moore et al. have reported the ORD in 1971 as part of an experimental study to determine the absolute configuration of (+)-1,2-cyclononadiene⁴⁵ (**9**). The ORD of bicyclic nonane precursors containing the structural motif of compound **6** was employed as evidence that **9** has an *R*-configuration. Because the OR is dominated by Rydberg excitations, calculations of the OR of **6** require diffuse functions as provided, for instance,

by the Vdiff basis. Further, in such a case it is advantageous to employ a Kohn–Sham potential with the correct asymptotic behavior.^{9,36} The SAOP belongs to this class of potentials and is seen to give a very accurate value for the excitation energy. A damping parameter of $\Gamma = 0.009$ yields almost perfect agreement with experiment for the magnitude of the OR near the excitation. One detail that is not reproduced accurately is the location of the longest wavelength where the OR changes sign, experimentally seen at about 220 nm. The calculation shows that this sign change occurs at around 240 nm, i.e., with an difference in energy of about 0.5 eV. Although this difference is within the error bars of TDDFT for calculations of excitation energies, the Cotton effect is obviously reproduced accurately by the calculations (centered around 187 nm). We have previously speculated that the sign change in a calculation without damping might have been red-shifted because of the too strong influence of the singularity nearby.⁹ However, the calculations with damping included suggest that this is not the (or not the only) reason because the crossover wavelength is only slightly closer to experiment. At present, the source of this discrepancy is unclear. A calculation of the OR using a preliminary version of a new code that considers a continuum model for *n*-pentane (which is presumably the solvent used for the experiments⁴⁵) did not shift the crossover point significantly. The Cotton effect of **6** at around 187 nm is negative. Because the sign of the OR is positive in the long wavelength limit, it must be dominated by higher energy transitions. However, the calculated $[\alpha]_{\text{D}}$ is larger than the experimental value (65.8 versus 42 deg/[dm (g/cm³)]). This indicates that the influence of positive higher-energy Cotton effects on the long-wavelength OR is overestimated. One might expect that this should blue shift the crossover point. It is possible that the use of a global damping parameter is beyond its limits when attempting to reproduce both the depth and the width of the trough simultaneously. Another source of error is the neglect of vibrational corrections to the ORD.⁵²

It is known that $[\alpha]_{\text{D}}$ for **6** is overestimated by about a factor of 3 when calculated with a basis without diffuse functions because of the influence of Rydberg states.⁹ Here, we have calculated a value of 122.7 deg/[dm (g/cm³)] with SAOP/TZP, compared to 65.8 with SAOP/Vdiff (see Supporting Information). The situation might be considered typical for small molecules without a chromophore such as a C=O or C=C group. It is interesting to investigate how the B3LYP hybrid functional performs for such a system. Figure 9 shows a comparison of SAOP/Vdiff with B3LYP/6-311++G** and experiment. It is seen that the lowest excitation energy is underestimated in the B3LYP calculation. The long-wavelength sign-change of the OR (exp. around 220 nm) is even further red-shifted than for SAOP/Vdiff. Our B3LYP/6-311++G** $[\alpha]_{\text{D}}$ is 48.6 deg/[dm (g/cm³)] (no damping). As an economic alternative to large high-quality diffuse basis sets, the aug-cc-pVDZ basis is also frequently chosen for optical rotation calculations.¹¹ With this basis, we obtain $+58.2$ deg/[dm (g/cm³)]. Both values agree well with results reported in ref 7 that were obtained with the B3LYP functional as implemented in the Gaussian code (aug-cc-pVDZ, 59.0 ; 6-311++G(2p,2d), 46.8). We calculated the ORD in the 180 – 250 nm region with both Gaussian-type basis sets but show only the 6-311++G** results because two curves were hardly distinguishable on the scale of the plot despite the fact that the $[\alpha]_{\text{D}}$ values differ noticeably. At 589.3 nm, the B3LYP results agree better with the experimental $[\alpha]_{\text{D}}$ of 42 deg/[dm (g/cm³)] than the SAOP/Vdiff result of 65.8 . However, in the resonance region between

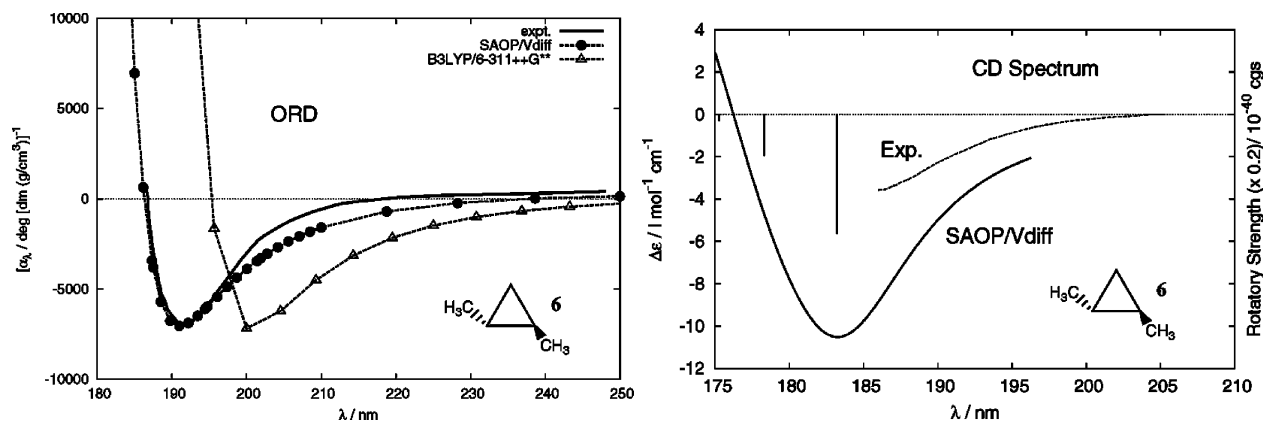


Figure 9. Left: ORD of compound **6**. Calculations at the SAOP/Vdiff and B3LYP/6-311++G** levels, using a damping parameter of $\Gamma = 0.009$ (0.24 eV). Right: CD of compound **6**. Calculation at the SAOP/Vdiff level. CD simulated with a Lorentzian broadening with a line width of $\Gamma = 0.009$ au (0.24 eV). Calculated excitation energies and rotatory strengths are indicated by vertical bars. Experimental data from ref 45.

180 and 250 nm the SAOP calculation is seen to be superior because of the better reproduction of the excitation energy. Therefore, we find that the performance of a functional in one wavelength range is not necessarily indicative of its performance at a different wavelength. Nonetheless, for the purpose of assigning the absolute configuration, the B3LYP calculation would be sufficiently accurate also in the resonance region.

The experimental study of **6** by Moore et al.⁴⁵ also reported CD. There is not very much data to compare with our calculations except for the sign and intensity of approximately half of a CD band. The wavelength around 187 nm, where the ORD changes sign, is not exactly located at the excitation energy, which is calculated to be at 183 nm (6.77 eV) at the SAOP/Vdiff level. We find a similar behavior when using the TZP basis. At the SAOP/TZP level the ORD changes sign at 183 nm. The lowest excitation energy is calculated at 6.95 eV (178 nm) at this level. The lack of experimental CD at wavelengths below about 185 nm does not allow us to make a direct comparison. Using the same line width of 0.009 au (0.24 eV) for the Lorentzian broadening of the CD as we used for calculating the ORD the simulated CD intensity for the SAOP/Vdiff calculation is too high. To improve the agreement with experiment for the CD, an even larger broadening would have to be applied. However, a larger broadening would yield less good agreement for the ORD. These results support our finding that a single (global) value for the damping parameter might not be able to accurately reproduce both the depth and the width of the ORD trough simultaneously with the same high accuracy.

Δ -[Co(en)₃]³⁺. The circular dichroism of the complex [Co(en)₃]³⁺ has been studied intensely over the past decades both experimentally and theoretically.⁵³ In many ways, [Co(en)₃]³⁺ has served as an antitype for a chiral metal complex, which makes it interesting in the context of the present study. The ORD in the visible wavelength range has been published already in 1937.⁵⁴ However, to our knowledge first-principles calculations have not yet been attempted. The Δ -configuration of the complex affords a negative Cotton effect in the visible range with a trough around 520 nm and a peak around 450 nm.

The CD spectrum of [Co(en)₃]³⁺ and other chiral Co and Rh complexes has been calculated previously using TDDFT.^{23,56,57} A discussion of the CD is beneficial to rationalize systematic errors obtained for the ORD in the visible range. Because the calculations in ref 23 were based on a different functional (the “BP” functional), we have repeated the calculations here with the revPBE functional based on the optimized structure of ref 23. We point out that the revPBE excitation energies and rotatory strengths are very similar to the BP results. The

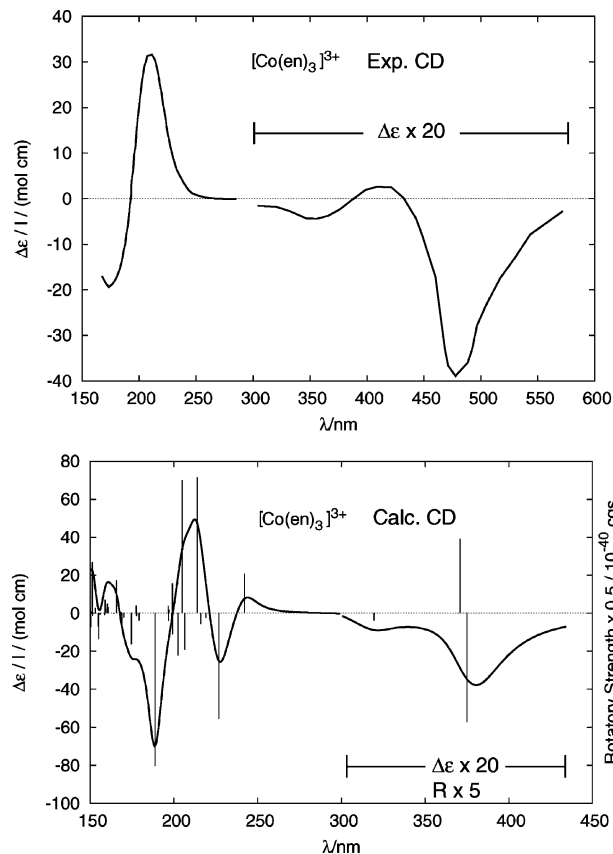


Figure 10. Circular dichroism of Δ -[Co(en)₃]³⁺. Calculation at the TZP/revPVE level. Experimental data from ref 55. Simulated CD spectrum based on a Lorentzian broadening with a line width of $\Gamma = 0.007$ au (0.2 eV). Calculated excitation energies and rotatory strengths are indicated by vertical bars.

simulated and the experimental CD spectrum are shown in Figure 10. We have used a global Lorentzian broadening with a line width of 0.007 au (0.2 eV) here to simulate the CD intensity, which leads to reasonable agreement with experiment for the low energy/long wavelength CD bands. The small positive CD band seen in the experimental spectrum around 430 nm is not due to an additional excitation. Depending on the type and width of the broadening, it is possible to reproduce this CD band in the simulations, but we have decided to keep the damping/broadening as consistent as possible throughout this work. A broadening of comparable line width as used here has previously also been applied in a study of the CD of group-8 tris-bidentate metal complexes, leading to overall reasonable

agreement with experiment.⁵⁸ The spectral features of the CD spectrum of $[\text{Co}(\text{en})_3]^{3+}$, basis set requirements, as well as systematic errors obtained in the calculations for the CD spectrum have been discussed extensively in ref 23 and shall not be repeated here. One of the findings of ref 23 was that the functional overestimates the energies of the formally “forbidden”⁵⁶ d-to-d transitions in this pseudo-octahedral complex. The corresponding CD bands are seen experimentally within the range 550–400 nm. At the same time, the energies of the intense charge-transfer CD transitions are underestimated in the calculations. The SAOP functional does not cure these deficiencies. However, the inclusion of solvent effects by means of the COSMO model improves the energies of the charge-transfer excitations considerably for this highly charged complex. See also ref 59 for an investigation of the $[\text{Co}(\text{en})_3]^{3+}$ CD spectrum based on the “discrete reaction field” solvent model⁶⁰ in conjunction with molecular dynamics simulations where similar solvent effects as well as some solvent broadening of the CD bands were obtained. Upon inclusion of solvent effects, the overall shape of the CD spectrum is qualitatively reproduced. For the charge-transfer region of the spectrum a significantly larger broadening would be necessary for better comparison with experiment because the simulated spectrum exhibits too much structure.²³ Mason et al. who published a CD spectrum for $[\text{Co}(\text{en})_3]^{3+}$ ⁵⁵ in 1976 estimated in an earlier study that the line width may increase roughly proportional to the square root of the excitation energy within the UV–vis range.⁶¹ Further, it is possible that some of the A_2/E symmetric pairs of charge-transfer transitions are underestimated in energy and exhibit too much of a splitting in the calculations.

Regarding conformational effects, fortunately the conformations of the chelate rings do not have a strong influence on the CD spectrum for $[\text{Co}(\text{en})_3]^{3+}$.²³ Thus, we restrict the discussion here to the ob_3 conformer of $[\text{Co}(\text{en})_3]^{3+}$, which has been found to be the most stable one in DFT calculations (see also ref 62).

With a qualitative agreement between computation and experiment being achieved for the CD spectrum, we may now proceed to a discussion of the ORD. The calculated and experimental ORD are displayed in Figure 11. Obviously, the Cotton effect in the visible range is caused by the d-to-d excitations in the complex. With an overestimation of the calculated energies of these transitions we thus expect a blue shift of the calculated ORD curve in comparison to experiment. This is indeed the case. The blue shift of the calculated ORD in the visible range corresponds to a 6000 cm^{-1} (0.74 eV) blue shift obtained for the d-to-d transitions in the CD.²³ Apart from this systematic error, which is well understood, the ORD is reproduced rather accurately. A tendency for an overestimation of the CD intensity in calculations of these types of metal complexes²³ appears to counterbalance an expected underestimation of the optical rotation at long wavelengths caused by the too high energies of the first few excitations. With a global damping parameter of 0.007 au the magnitude of the trough and the peak are reasonably well reproduced. We conclude that also for this transition metal complex a calculation of the ORD in the resonance region would qualify for an assignment of the absolute configuration if it were not known. The blue shift of the ORD and other systematic errors in the computation that might affect the quality of the calculated ORD can be further studied by an additional comparison of the calculated CD with experiment. A comparative study of the ORD with hybrid and nonhybrid functionals is beyond the scope of the present paper and will be left for future studies. In contrast to organic molecules the success of hybrid DFT for linear

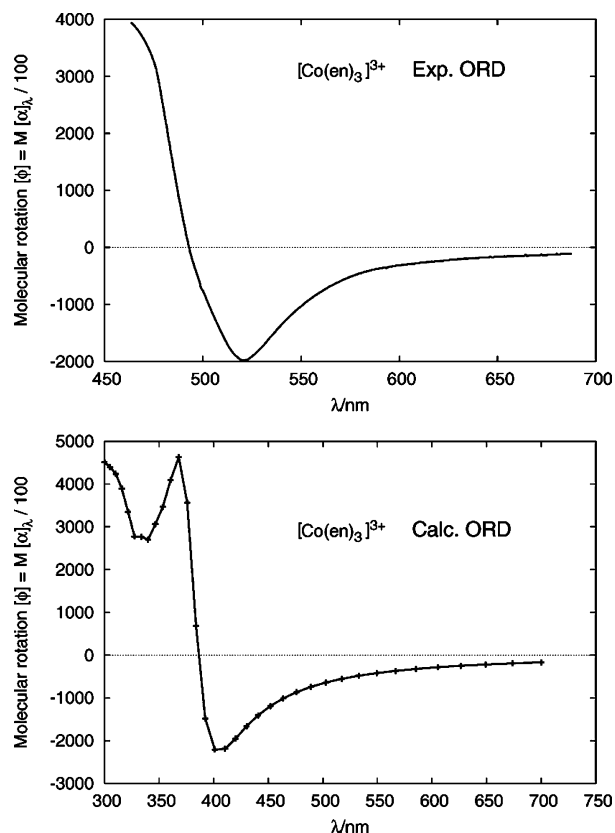


Figure 11. Optical rotatory dispersion of Δ - $[\text{Co}(\text{en})_3]^{3+}$. Calculation at the TZP/revPVE level. Experimental data from ref 54.

response properties in general, and of optical activity in particular, has not been demonstrated conclusively for 3d transition metal complexes.^{58,63} One of the reasons is a delicate interplay between structure and property.^{58,64}

4. Conclusions

One goal of the present work has been to explore to which extent DFT calculations with relatively small basis sets are able to obtain *reasonable* ORD curves for fast routine applications to absolute configuration assignments. For this purpose, even comparatively large differences between theory and experiment are acceptable at any particular wavelength as long as the overall shape and order of magnitude of the ORD agrees with experiment and the excitation energies are reasonably well reproduced. Except for some functional specific deficiencies mainly for Tröger’s base **5** and to some extent for $[\text{Co}(\text{en})_3]^{3+}$, the agreement of the DFT calculations with experiment is indeed very reasonable for the molecules studied here. We have shown that the application of a global damping parameter of the order of 0.2 eV (0.007 au) in the calculation leads to a realistic behavior of the ORD in the vicinity of an excitation. For molecules with excitations in the UV/vis range the anomalous dispersion of the optical rotation might therefore be a useful tool for an unambiguous assignment of the absolute configuration.

For Tröger’s base (**5**), the calculations lead to reasonable agreement with experiment for wavelengths down to about 350 nm. Between 250 and 350 nm, the OR is influenced by several Cotton effects of varying sign and magnitude and therefore difficult to reproduce. One of the problematic factors is the energetic proximity of strong CD transitions in this energy range. However, even for **5**, the inclusion of damping is seen to be clearly advantageous in analyzing this complicated situation.

A calculation without damping leads to wildly changing optical rotations with huge magnitudes that cannot be directly compared to experiment. In this case, it is difficult to assess the accuracy of the computational method.

A comparison of a calculated CD spectrum with experiment may reveal additional information about how the approximations in the calculations influence the optical rotation. Stephens et al. have recently also pointed out the advantage of using *both* CD and OR calculated at the same level of theory for configurational assignments.¹² With the basis sets employed in this work, it is straightforward and computationally affordable to calculate at least a few CD transitions for molecules of the size studied here. We have seen that for Tröger's base (**5**) the CD calculations reveal critical information about the energy of the excitations and the sign of their CD. For the metal complex [Co(en)₃]³⁺ (**7**) a comparison of both CD and ORD with experiment has also turned out to be beneficial. The calculated ORD agrees quite well with experiment except for a blue shift that can be traced back to an overestimation of the energies of the d-to-d transition in the complex.

We believe that the present study demonstrates that efficient time-dependent DFT calculations of optical rotatory dispersion in the resonance region can support the assignment of absolute configurations of chiral molecules. Depending on the nature of the transitions and the overall size of the molecule, a qualitatively correct ORD sign pattern can sometimes be obtained even without employing large multiply polarized diffuse basis sets. However, in this case large relative errors for the OR at any given individual wavelength must be expected. A combination of measurements and calculations of the ORD as well as the CD spectrum would provide sufficient theoretical information to be able to make an assignment of the absolute configuration with high confidence. In problematic cases, such as Tröger's base (**5**), the combination of CD and ORD might also reveal which of the wavelength ranges could be problematic for a configurational assignment and in which way one might be able to improve the calculations.

Improved accuracy of the calculations might be achieved by applying a vibrational averaging to the optical rotation and by considering solvent effects. We have shown recently that in DFT calculations zero-point vibrational (ZPV) corrections can amount to about 25% of the equilibrium value for D-line optical rotations for rigid organic molecules⁵² and might be significantly larger in select cases. The ZPV corrections might also exhibit a pronounced dispersion, as was recently demonstrated for methyloxirane.⁶⁵

Acknowledgment. We thank the Center for Computational Research (CCR) at the University of Buffalo for support. J.A. acknowledges the CAREER program of the National Science Foundation (grant no. CHE-0447321) as well as the Petroleum Research Fund for financial support of his research. L.J. and G.C.S. thanks the Air Force Office of Scientific Research MURI program (F49620-02-1-0381).

Supporting Information Available: ORD for molecules **1–5** calculated with the revPBE functional and the TZP basis; lowest 5 CD transition for molecules **1** to **5** calculated at the SAOP/TZP level; specific rotation of all molecules at 589.3 nm; calculated CD spectra for molecules **2** and **3** showing the individual transitions and their rotatory strengths; complete ref 19.

References and Notes

(1) Polavarapu, P. L.; Chakraborty, D. K. *J. Am. Chem. Soc.* **1998**, *120*, 6160–6164.

- (2) Kondru, R. K.; Wipf, P.; Beratan, D. N. *J. Am. Chem. Soc.* **1998**, *120*, 2204–2205.
- (3) Crawford, D. T.; Owens, L. S.; Tam, M. C.; Schreiner, P. R.; Koch, H. *J. Am. Chem. Soc.* **2005**, *127*, 1368–1369.
- (4) Giorgio, E.; Viglione, R. G.; Zanasi, R.; Rosini, C. *J. Am. Chem. Soc.* **2004**, *126*, 12968–12976.
- (5) Rinderspacher, B. C.; Schreiner, P. R. *J. Phys. Chem. A* **2004**, *108*, 2867–2870.
- (6) Stephens, P. J.; Devlin, F. J.; Cheeseman, J. R.; Frisch, M. J.; Bortolini, O.; Besse, P. *Chirality* **2003**, *15*, S57–S64.
- (7) Stephens, P. J.; Devlin, F. J.; Cheeseman, J. R.; Frisch, M. J. *J. Phys. Chem. A* **2001**, *105*, 5356–5371.
- (8) Grimme, S. *Chem. Phys. Lett.* **2001**, *339*, 380–388.
- (9) Autschbach, J.; Ziegler, T.; Patchkovskii, S.; van Gisbergen, S. J. A.; Baerends, E. J. *J. Chem. Phys.* **2002**, *117*, 581–592.
- (10) Polavarapu, P. L. *Chirality* **2002**, *14*, 768–781.
- (11) Syphens, P. J.; McCann, D. M.; Cheeseman, J. R.; Frisch, M. J. *Chirality* **2005**, *17*, S52–S64.
- (12) Stephens, P. J.; McCann, D. M.; Butkus, E.; Stoncius, E.; Cheeseman, J. R.; Frisch, M. J. *J. Org. Chem.* **2004**, *69*, 1948–1958.
- (13) Polavarapu, P. L.; Zhao, C. *J. Am. Chem. Soc.* **1999**, *121*, 246–247.
- (14) Moscovitz, A. *Adv. Chem. Phys.* **1962**, *4*, 67–112.
- (15) Polavarapu, P. L. *J. Phys. Chem. A* **2005**, *109*, 7013–7023.
- (16) Djerassi, C. *Optical Rotatory Dispersion*; McGraw-Hill: New York, 1960.
- (17) Norman, P.; Bishop, D. M.; Jensen, H. J. A.; Oddershede, J. *J. Chem. Phys.* **2001**, *115*, 10323–10334.
- (18) Norman, P.; Ruud, K.; Helgaker, T. *J. Chem. Phys.* **2004**, *120*, 5027–5035.
- (19) Baerends, E. J.; et al. "Amsterdam Density Functional", Theoretical Chemistry, Vrije Universiteit, Amsterdam, URL <http://www.scm.com>.
- (20) van Gisbergen, S. J. A.; Fonseca-Guerra, C.; Baerends, E. J. *J. Comput. Chem.* **2000**, *21*, 1511–1523.
- (21) Krykunov, M.; Autschbach, J. *J. Chem. Phys.* **2005**, *123*, 114103–10.
- (22) Jensen, L.; Autschbach, J.; Schatz, G. C. *J. Chem. Phys.* **2005**, *122*, 224115–11.
- (23) Autschbach, J.; Jorge, F. E.; Ziegler, T. *Inorg. Chem.* **2003**, *42*, 2867–2877.
- (24) Krykunov, M.; Banerjee, A.; Ziegler, T.; Autschbach, J. *J. Chem. Phys.* **2005**, *122*, 074105–7.
- (25) Dobson, J. F.; Vignale, G.; Das, M. P., Eds. *Electronic density functional theory. Recent progress and new directions*; Plenum Press: New York, 1998.
- (26) Gross, E. K. U.; Dobson, J. F.; Petersilka, M. *Top. Curr. Chem.* **1996**, *181*, 81–172.
- (27) Casida, M. E. Time-dependent density functional response theory for molecules. In *Recent advances in density functional methods*, Vol. 1; Chong, D. P., Ed.; World Scientific: Singapore, 1995.
- (28) Autschbach, J.; Ziegler, T. *J. Chem. Phys.* **2002**, *116*, 891–896.
- (29) Grimme, S.; Furche, F.; Ahlrichs, R. *Chem. Phys. Lett.* **2002**, *361*, 321–328.
- (30) Buckingham, A. D. *Adv. Chem. Phys.* **1967**, *12*, 107–142.
- (31) Autschbach, J.; Ziegler, T.; van Gisbergen, S. J. A.; Baerends, E. J. *J. Chem. Phys.* **2002**, *116*, 6930–6940.
- (32) Perdew, J. P.; Burke, K.; Ernzerhof, M. *Phys. Rev. Lett.* **1996**, *77*, 3865–3868.
- (33) Zhang, Y.; Yang, W. *Phys. Rev. Lett.* **1998**, *80*, 890.
- (34) Perdew, J. P.; Burke, K.; Ernzerhof, M. *Phys. Rev. Lett.* **1998**, *80*, 891.
- (35) Hammer, B.; Hansen, L. B.; Norskov, J. K. *Phys. Rev. B* **1999**, *59*, 7413–7421.
- (36) Schipper, P. R. T.; Gritsenko, O. V.; van Gisbergen, S. J. A.; Baerends, E. J. *J. Chem. Phys.* **2000**, *112*, 1344–1352.
- (37) Tozer, D. J.; Handy, N. C. *J. Chem. Phys.* **1998**, *109*, 10180–10189.
- (38) Grüning, M.; Gritsenko, O. V.; van Gisbergen, S. J. A.; Baerends, E. J. *J. Chem. Phys.* **2001**, *114*, 652–660.
- (39) te Velde, G.; Baerends, E. J. *J. Comput. Phys.* **1992**, *99*, 84.
- (40) Klamt, A.; Schüürmann, G. *J. Chem. Soc., Perkin Trans. 2* **1993**, 799–805.
- (41) Pye, C. C.; Ziegler, T. *Theor. Chem. Acc.* **1999**, *101*, 396–408.
- (42) Dalton, a molecular electronic structure program, Release 2.0 2005, see <http://www.kjemi.uio.no/software/dalton/dalton.html>.
- (43) Becke, A. D. *J. Chem. Phys.* **1993**, *98*, 5648–5652.
- (44) Furche, F.; Ahlrichs, R.; Wachsmann, C.; Weber, E.; Sobanski, A.; Vögtle, F.; Grimme, S. *J. Am. Chem. Soc.* **2000**, *122*, 1717–1724.
- (45) Moore, W. R.; Anderson, H. W.; Clark, S. D.; Ozretich, T. M. *J. Am. Chem. Soc.* **1971**, *93*, 4932–4934.
- (46) Pulm, F.; Schramm, J.; Hormes, J.; Grimme, S.; Peyerimhoff, S. *Chem. Phys.* **1997**, *224*, 143–155.

- (47) Neugebauer, J.; Baerends, E. J.; Nooijen, M.; Autschbach, J. *J. Chem. Phys.* **2005**, *122*, 234305–7.
- (48) Takeya, K.; Itokawa, H. *Chem. Pharm. Bull.* **1977**, *25*, 1947–1951.
- (49) Hirata, T. *Bull. Chem. Soc. Jpn.* **1972**, *45*, 3458–3464.
- (50) Giorgio, E.; Minichino, C.; Viglione, R. G.; Zanasi, R.; Rosini, C. *J. Org. Chem.* **2003**, *68*, 5186–5192.
- (51) Mason, S. F.; Vane, G. W.; Schofield, K.; Wells, R. J.; Whitehurst, J. S. *J. Chem. Soc. B* **1967**, 553–556.
- (52) Mort, B. C.; Autschbach, J. *J. Phys. Chem. A* **2005**, *109*, 8617–8623.
- (53) Kuroda, R.; Saito, Y. Circular dichroism of inorganic complexes: Interpretation and applications. In *Circular Dichroism. Principles and Applications*; Nakanishi, K., Berova, N., Woody, R. W., Eds.; VCH: New York, 1994.
- (54) Lehl, H.; Buschbeck, K.-C.; Gagarin, R. Kobalt B/2. In *Gmelins Handbuch der Anorganischen Chemie*; Verlag Chemie: Weinheim, 1964.
- (55) Mason, S. F.; Seal, R. H. *Mol. Phys.* **1976**, *31*, 755–775.
- (56) Jorge, F. E.; Autschbach, J.; Ziegler, T. *Inorg. Chem.* **2004**, *42*, 8902–8910.
- (57) Jorge, F. E.; Autschbach, J.; Ziegler, T. *J. Am. Chem. Soc.* **2005**, *127*, 975–985.
- (58) Le Guennic, B.; Hieringer, W.; Görling, A.; Autschbach, J. *J. Phys. Chem. A* **2005**, *109*, 4836–4846.
- (59) Jensen, L.; Swart, M.; van Duijnen, P. T.; Autschbach, J. *Int. J. Quantum Chem.*, in press.
- (60) Jensen, L.; van Duijnen, P. T.; Snijders, J. *J. Chem. Phys.* **2003**, *119*, 3800–3809.
- (61) Brown, A.; Kemp, C. M.; Mason, S. F. *J. Chem. Soc. A* **1971**, 751–755.
- (62) Freedman, T. B.; Cao, X.; Young, D. A.; Nafie, L. A. *J. Phys. Chem. A* **2002**, *106*, 3560–3565.
- (63) Rosa, A.; Ricciardi, G.; Gritsenko, O.; Baerends, E. J. Excitation energies of metal complexes with time-dependent density functional theory. In *Principles and Applications of Density Functional Theory in Inorganic Chemistry I*, Vol. 112; Kaltsoyannis, N., McGrady, J. E., Eds.; Springer: Heidelberg, 2004.
- (64) Hieringer, W.; Görling, A.; Arbouznikov, A. To be published.
- (65) Ruud, K.; Zanasi, R. *Angew. Chem., Int. Ed.* **2005**, *44*, 3594–3596.